Published in final edited form as:
*Nano Lett*. 2008 November ; 8(11): 3834–3838. doi:10.1021/nl802223f.

# High Contrast *In vitro* and *In vivo* Photoluminescence Bioimaging Using Near Infrared to Near Infrared Up-Conversion in $Tm^{3+}$ and $Yb^{3+}$ Doped Fluoride Nanophosphors

**Marcin Nyk**, **Rajiv Kumar**, **Tymish Y. Ohulchanskyy**, **Earl J. Bergey**, and **Paras N. Prasad**[*]
Institute for Lasers, Photonics and Biophotonics, Department of Chemistry, University at Buffalo, State University of New York, Buffalo, New York 14260

## Abstract

A new approach for photoluminescence imaging *in vitro* and *in vivo* has been shown, utilizing near infrared to near infrared (NIR-to-NIR) up-conversion in nanophosphors. This NIR-to-NIR up-conversion process provides deeper light penetration into biological specimen and results in high contrast optical imaging due to absence of an autofluorescence background and decreased light scattering. Aqueous dispersible fluoride ($NaYF_4$) nanocrystals (20–30 nm size) co-doped with the rare earth ions, $Tm^{3+}$ and $Yb^{3+}$, were synthesized and characterized by TEM, XRD and photoluminescence (PL) spectroscopy. *In vitro* cellular uptake was shown by the PL microscopy visualizing the characteristic emission of $Tm^{3+}$ at ~ 800 nm excited with 975 nm. No apparent cytotoxicity was observed. Subsequent animal imaging studies were performed using Balb-c mice injected intravenously with up-converting nanophosphors, demonstrating the high contrast PL imaging *in vivo*.

### Keywords

Nanophosphors; Energy Up-conversion; Near Infrared *In vitro* and *In vivo* imaging

Fluorescence optical imaging is an important technique for biomedical applications due to its high sensitivity and resolution.[1–3] With the advent of confocal and two photon excited fluorescence microscopy, one can now obtain detailed information on cellular interactions and dynamics.[4–7] Traditionally, organic fluorophores are used in imaging of cells and tissues.[6–9] Among the key considerations for the fluorescent probes for *in vitro* and *in vivo* imaging are: (i) emission quantum efficiency; (ii) excitation/emission wavelength to minimize imaging background, (iii) increased photostability and (iv) combined applicability in confocal/multiphoton microscopy and whole body optical imaging systems. The "optical transmission window" of the biological tissues in near-infrared (NIR) range (750–1000 nm)[1,3] allows for deeper light penetration and results in lower autofluorescence and reduced light scattering, thus producing increased image contrast. Therefore, probes which are excitable in NIR range are preferable for both *in vitro* and *in vivo* imaging. These considerations have lead to intensive research in the development of fluorophores which can be efficiently excited in the NIR range using single or two-photon excitation.[1] However,

[*]CORRESPONDING AUTHOR FOOTNOTE Dr. Paras N. Prasad Distinguished Professor Institute for Lasers, Photonics and Biophotonics 428 Natural Sciences Complex The State University of New York University at Buffalo Buffalo, NY 14260-3000 pnprasad@buffalo.edu Phone: 716-645-6800 ext.2099 Fax: 716-645-6945.

SUPPORTING INFORMATION: Scheme of the energy levels of $Yb^{3+}$ and $Tm^{3+}$ doped in $NaYF_4$ nanocrystals, details of *in vivo* experimental setup, cell viability assay for nanophosphors. This material is available free of charge via the Internet at http://pubs.acs.org.

NIR absorbing organic fluorophores are more susceptible to photobleaching and lack emission efficiency. For two-photon imaging, nonlinear excitation requires the use of expensive short pulsed lasers (e.g. Ti-sapphire femtosecond pulsed lasers). Both single and two photon absorbing fluorophores also have broad emission spectra, therefore, limiting their ability for multiplexed imaging. Furthermore, no systems are currently available for whole body imaging using two-photon excitation.

Recent developments of quantum dots (QDs) and quantum rods (QRs) for bioimaging have brought a new dimension to bioimaging.[10–12] QDs are photoluminescent nanocrystals demonstrating size dependent absorption and emission spectra in the visible and NIR ranges. The emission wavelength of these nanocrystals can be tuned by changing size and aspect ratios. They are more stable against photobleaching than organic fluorophores and have narrower emission spectra. These narrow emission spectra make them more suitable for multiplexed imaging.[13] However, due to low absorbance intensity of the first excitonic absorption band and small Stokes shift between absorption and emission, NIR emitting QDs can be only efficiently excited in visible range, which significantly limits their application in *in vivo* imaging. In addition, there is a wide concern about the toxicity of these QDs owing to the presence of heavy metals in their composition.[14,15]

In this communication, we report a new approach for high contrast, photoluminescence (PL) imaging that utilizes NIR-to-NIR up-conversion (UC) transition in $Tm^{3+}$ and $Yb^{3+}$ doped fluoride nanophosphors (UCNPs). Optical up-conversion in rare-earth ($RE^{3+}$) ions involves excitation by two or more photons to reach a higher excited energy level from which emission occurs.[16] An up-conversion process is much more efficient in comparison to two-photon absorption because of an existing intermediate energy level due to which up-conversion process is sequential, as opposed to a virtual intermediate level in the case of two-photon absorption, where the process is simultaneous. Thus an up-conversion process requires much lower excitation intensity which allows the use of inexpensive and readily available continuous wave (CW) laser diodes against expensive femtosecond pulsed lasers needed for simultaneous two-photon excitation.[17] Another important feature of $RE^{3+}$ emitters is their characteristically narrow PL spectra.[18] Optical properties of the $RE^{3+}$ doped nanophosphors are independent of particle size and emission can be tuned by doping with different lanthanide ions. The most extensively studied up-conversion process is with $Er^{3+}$, in which a 975 nm excitation produces emission in green (peaks at 520, 538, 550 nm) and red (peaks at 649, 653, 667 nm) spectral ranges.[19,20] Up-converting nanophosphors doped with $Er^{3+}$ have recently been used for bioimaging.[21–22]

The advantage offered by PL imaging with up-converting nanophosphors (UCNPs) reported here is that both the excitation wavelength of 975 nm and the up-converted emission at around 800 nm are in the NIR range, which is an ideal case for deeper tissue penetration. Up-conversion PL imaging provides remarkably high optical contrast because of absence of autofluorescence and decreased light scattering. Due to the quasi-quadratic dependence of the PL intensity on the power of excitation of the UCNPs,[23] there is an inherent 3-D localization of PL, similar to two-photon induced fluorescence, which can be used in the development of 3-D imaging systems.

The synthesis of UCNPs was carried out as described previously, with some modifications.[23,24] In a typical synthesis fixed amounts of commercial $Tm_2O_3$, $Yb_2O_3$ and $Y_2O_3$ were mixed and solubilized in 50 % concentrated trifluoroacetic acid at 80°C and slowly evaporated to dryness in vacuum oven at 70°C. The molar compositions of the feed external solution were [Tm/(Tm+Yb+Y)] = 0.02 and [Yb/(Tm+Yb+Y)] = 0.2. Next, the obtained trifluoroacetate precursor salt was added to a three-necked flask containig 30 ml octadecane, 30 ml oleic acid and 4.5 mmol of sodium trifluoroacetate. The molar ratio of

$Na(CF_3COO)$ to $RE(CF_3COO)$ was kept 1.8 to form the pure cubic phase of $\alpha$-$NaREF_4$. The solution was heated to 110°C under vacuum with stirring for ~30 min. To remove water and oxygen, the flask was purged with dry nitrogen at 10 min. intervals. The yellow solution was then heated to 300 °C under nitrogen and vigorous stirring for 1 h. The mixture was cooled to room temperature and precipitated by acetone in an ultrasonic bath and collected by centrifugation at 11,000 rpm for 30 min. The precipitate was washed with ethanol and the nanocrystals were dispersed in 4 ml chloroform. Aqueous dispersion of the nanocrystals was accomplished by diluting 2 ml of the chloroform dispersion with 3 ml of chloroform and incubating with 5 ml of 3-mercaptopropionic acid. After stirring overnight, 5 ml of HPLC grade water was added and stirred for 30 min. The turbid solution obtained was centrifuged and the pellet was redispersed in 5 ml of HPLC grade water by sonication. Finally the aqueous dispersion of the $NaYF_4$:$Tm^{3+}$,$Yb^{3+}$ UCNPs was filtered with a 0.4 μm syringe filter and stored at 4 °C for future use.

The dimension and morphology characterizations of the nanocrystals were performed by transmission electron microscopy (TEM), using a JEOL model JEM–100CX microscope at an acceleration voltage of 80 kV. The water dispersed UCNPs were uniform in size with a very narrow size distribution, as shown by the TEM picture (Figure 1). Overall phase compositions of the samples were determinated by X-ray powder diffraction with a Siemens D500 diffractometer using $CuK_{\alpha 1}$ radiation, $\lambda$=0.154 nm. Figure 2 shows the XRD patterns of the UCNPs showing diffraction lines that can be ascribed to the face-centered cubic $NaYF_4$ structure (JCPDS#77-2042). By using the Scherrer's equation,[25] the average size of the crystallite grains was determined from all the reflections to be ca. 20 nm.

Photoluminescence (PL) spectroscopy was performed using a Fluorolog-3.11 spectrofluorometer (Jobin Yvon), using excitation from a laser diode emitting at 975 nm (Qphotonics). The PL spectrum of the aqueous dispersion of UCNPs showed characteristic multiple narrow spectral bands of $Tm^{3+}$ (Figure 3) which is attributed to the fact that the 4f electrons in $RE^{3+}$ ions are effectively shielded from surrounding crystal fields because of the filled outer shells of $5s^2$ and $5p^6$ electrons.[18] The $Yb^{3+}$ ions, excited with 975 nm, transfer energy to $Tm^{3+}$, which results in the characteristic $Tm^{3+}$ emission bands at 479, 648 and 800 nm. The visible blue PL peak is a radiative deactivation of the $^1G_4$ to the $^3H_6$ energy levels of $Tm^{3+}$, whereas the NIR peak at 800 nm corresponds to the $^3H_4 \rightarrow {}^3H_6$ transition; both levels are populated through the $^2F_{5/2}$ level of $Yb^{3+}$, thus up-converting the energy.[23]

To determine whether UCNPs can be used for cellular imaging, we have performed *in vitro* cellular studies using human pancreatic cancer cells, Panc 1. The cells were cultured in Dulbecco minimum essential media (MEM-α) with 10 % fetal bovine serum (FBS), 1 % penicillin, and 1 % amphotericin B. The day before treatment, cells were seeded in 35 mm culture dishes. On treatment day, an aqueous dispersion of UCNPs was added to the cells (confluence of 70–80 %), which were incubated for two hours at 37 °C. Cellular imaging was done using a Nikon Eclipse TE 2000 microscope equipped with the Nuance GNIR CCD camera (Cambridge Research & Instrumentation Inc., CRi), which is capable of imaging in the range of 500–950 nm. A fiber coupled laser diode (Qphotonics) emitting at 975 nm was used as the light source and the fiber was introduced through the entrance port of the microscope. Figure 4 shows the transmission and PL images of Panc 1 cells treated with the UCNPs fallowing excitation at 975 nm. The localized emission spectrum acquired from the cells showed the characteristic photoluminescence of $Tm^{3+}$ peaked at ~ 800 nm (Figure 4, inset). Complete absence of autofluorescence confirms the capability of UCNPs for high contrast PL imaging of cells, *in vitro*. It is worth noting that this PL imaging shows the inherent three-dimensional localization feature, similar to that obtained with two-photon excited fluorescence.[1,26] This is due to the quasi-quadratic dependence of the PL intensity on the power of excitation.[23] As can be seen in Figure 5, no overt toxicity of the

nanoparticles was found using the MTS cell viability assay (see supporting information for details).

To demonstrate suitability of $NaYF_4$:$Tm^{3+}$,$Yb^{3+}$ UCNP for *in vivo* imaging, we injected Balb C mice intravenously (tail vein) with UCNPs (200 ul of 2 mg/ml NPs in water with 5 % glucose) and imaged 2 hrs post injection. *In vivo* PL imaging was accomplished using the Maestro GNIR FLEX fluorescence imaging system (CRi) (for details, see supporting information). The UCNPs were excited at 975 nm by the defocused emission from the fiber coupled laser diode introduced into imaging chamber. An emission filter (850 SP) in front of the imaging CCD camera was used to cut off the excitation light.

Figure 6 presents the *in vivo* Maestro whole-body images of a Balb-C mouse injected with the UCNPs. The spectrally unmixed, high contrast images clearly demonstrate the feasibility to image and spectrally distinguish the characteristically emitting UCNPs (shown as red), using the Maestro imaging software. A scan in the range of 700 to 850 nm showed an intense NIR luminescence peaking at ~ 800 nm. The signal was readily detectable both through the skin (without hair removal) and after dissection of the animal. In Figure 6, the images show saturated levels of PL in the liver and the spleen, indicating a high uptake of UCNPs by these organs. The high contrast between the background and the PL signal for UCNPs is the result of NIR to NIR up-conversion PL imaging. It is worth nothing that the UCNPs showed no overt short-term toxicity in the injected mice after 48 hrs post-injection.

In conclusion, we have synthesized and characterized the NIR-to-NIR UCNPs. We have demonstrated that these UCNPs possess the essential features required for both *in vitro* and *in vivo* bioimaging applications. These include: (i) colloidal stability in water, (ii) efficient NIR up-conversion PL emission with characteristically sharp spectral lines excitable in the NIR range (975 nm). UCNPs do not need the high excitation intensity, which is required for simultaneous two-photon excitation of organic dyes or QDs used for two-photon microscopy. This makes the process much more efficient in comparison to direct two-photon absorption[27] and allows excitation and imaging of UCNPs using readily available and less expensive low-power continuous wave laser diodes. We have shown here that this novel approach using NIR-to-NIR UCNPs enables high contrast cellular and tissue imaging with no overt indication of toxicity. This study provides a foundation for the development of 3-D imaging systems for the advanced whole body optical imaging.

## Supplementary Material

Refer to Web version on PubMed Central for supplementary material.

## Acknowledgments

This work was supported by grants from the National Institute of Health (R01CA119358-01 and RO1CA104492) and the John R. Oishei Foundation. We thank Dr. Indrajit Roy for useful discussions.

## REFERENCES

(1). Prasad, PN. Introduction to Biophotonics. Wiley-Interscience; New York: 2003. p. 593

(2). Sharma P, Brown S, Walter G, Santra S, Moudgil B. Adv Colloid Interface Sci. 2006; 123–126:471–85.

(3). Weissleder R. Nat Biotechnol. 2001; 19(4):316–317. [PubMed: 11283581]

(4). Michaelis J, Hettich C, Mlynek J, Sandoghdar V. Nat. Med. 2000; 405(6784):586–590.

(5). Rudolph W, Kempe M. J. Mod. Optics. 1997; 44(9):1617–1642.

(6). Lakowicz, JR. Principles of fluorescence spectroscopy. 2nd ed.. Kluwer; New York: 1999.

(7). Periasamy, A. Methods in Cellular Imaging. Oxford University Press; New York: 2001.

(8). Ow H, Larson DR, Srivastava M, Baird BA, Webb WW, Wiesner U. Nano Lett. 2005; 5(12):113–117. [PubMed: 15792423]

(9). Zhao X, Tapec-Dytioco R, Tan W. J. Am. Chem. Soc. 2003; 125(38):11474–11475. [PubMed: 13129331]

(10). Alivisatos AP. Nat. Biotechnol. 2004; 22(1):47–52. [PubMed: 14704706]

(11). Ruan G, Agrawal A, Marcus AI, Nie S. J. Am. Chem. Soc. 2007; 129(47):14759–14766. [PubMed: 17983227]

(12). Yong K-T, Qian J, Roy I, Lee HH, Bergey EJ, Tramposch KM, He S, Swihart MT, Maitra A, Prasad PN. Nano Lett. 2007; 7(3):761–765. [PubMed: 17288490]

(13). Han M, Gao X, Su JZ, Nie S. Nat. Biotechnol. 2001; 19:631–635. [PubMed: 11433273]

(14). Hardman R. Environ. Health Perspect. 2006; 114:165–172. [PubMed: 16451849]

(15). Male KB, Lachance B, Hrapovic S, Sunahara G, Luong JHT. Anal. Chem. 2008; 80:5487–5493. [PubMed: 18553941]

(16). Prasad, PN. Nanophotonics. Wiley-Interscience; New York: 2004.

(17). Heer S, Kompe K, Gudel HU, Haase M. Adv. Mater. 2004; 16(23–24):2102–2105.

(18). Kenyon AJ. Prog. Quant. Electron. 2002; 26:225–284.

(19). Schafer H, Ptacek P, Kompe K, Haase M. Chem. Mater. 2007; 19(6):1396–1400.

(20). Chen XY, Ma E, Liu GK. J. Phys. Chem. C. 2007; 111(28):10404–10411.

(21). Lim SF, Riehn R, Ryu WS, Khanarian N, Tung CK, Tank D, Austin RH. Nano Lett. 2006; 6(2): 169–174. [PubMed: 16464029]

(22). Chatterjee DK, Rufaihah AJ, Zhang Y. Biomaterials. 2008; 29(7):937–943. [PubMed: 18061257]

(23). Boyer J-C, Cuccia LA, Capobianco JA. Nano Lett. 2007; 7(3):847–852. [PubMed: 17302461]

(24). Zhang YW, Sun X, Si R, You LP, Yan CH. J. Am. Chem. Soc. 2005; 127(10):3260–3261. [PubMed: 15755126]

(25). Klug, P.; Alexander, LE. X-ray Diffraction Procedure. Wiley; New York: 1954.

(26). So PTC, Dong CY, Master BR, Berland KM. Annu. Rev. Biomed. Eng. 2000; 2:399–429. [PubMed: 11701518]

(27). Heer S, Kömpe K, Gudel HU, Haase M. Adv. Mat. 2004; 16(23–24):2102–2105.

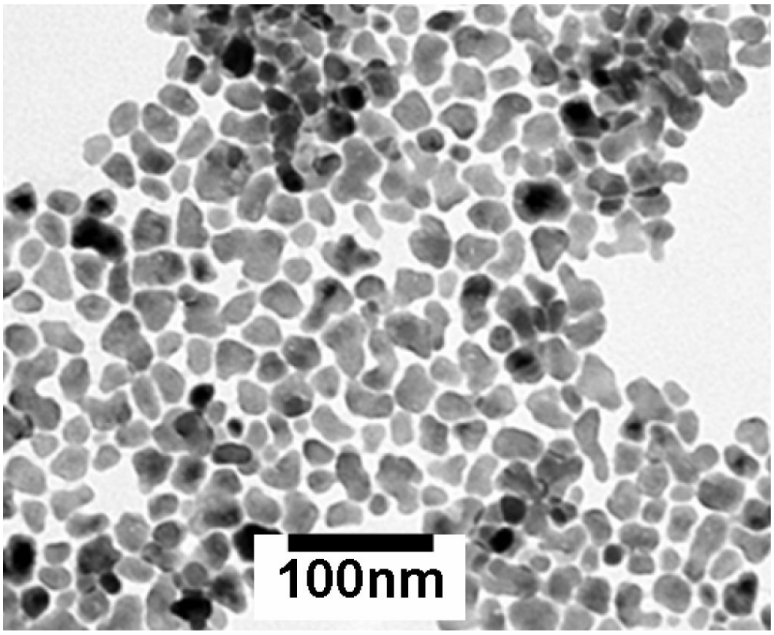


**Figure 1.**
TEM micrograph of $NaYF_4$:2%$Tm^{3+}$, 20%$Yb^{3+}$ UCNPs showing the size uniformity of the particles.

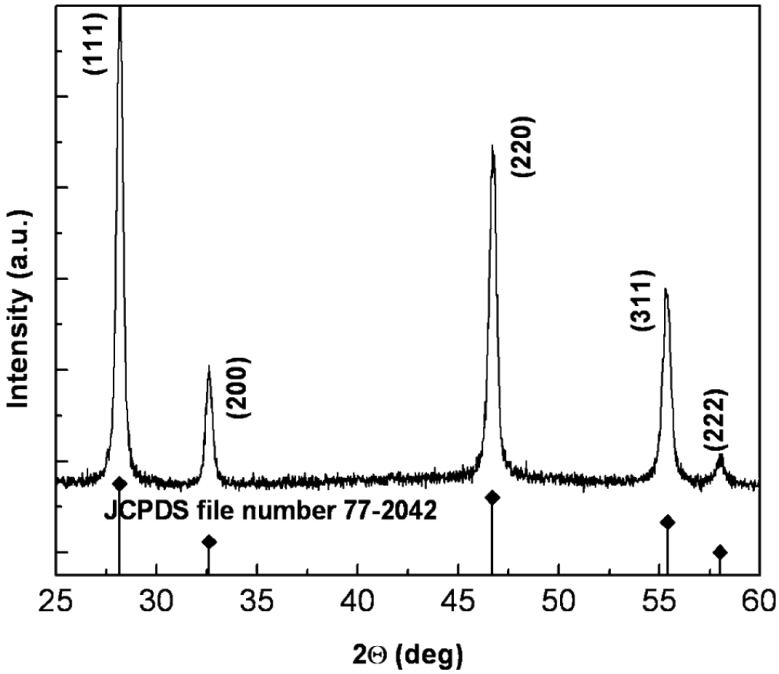


**Figure 2.**

X-ray diffraction patterns of $NaYF_4$:2%$Tm^{3+}$, 20%$Yb^{3+}$ UCNPs. The JCPDS#77-2042 line pattern for α-$NaYF_4$ (bottom plot) is shown for reference.

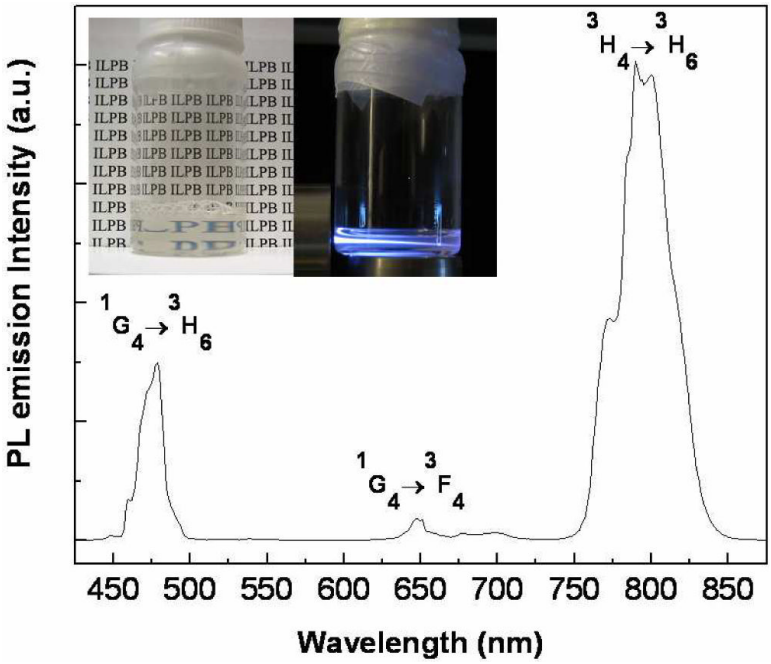


**Figure 3.**

Photoluminescence spectra of NaYF :2%$Tm^{3+}$,20%$Yb^{3+}$ UCNPs in aqueous dispersion; excitation at 975 nm. Inset: sample of the UCNPs aqueous dispersion demonstrating colloidal stability, optical transparency and efficient visible (blue) PL under excitation with 975 nm. .

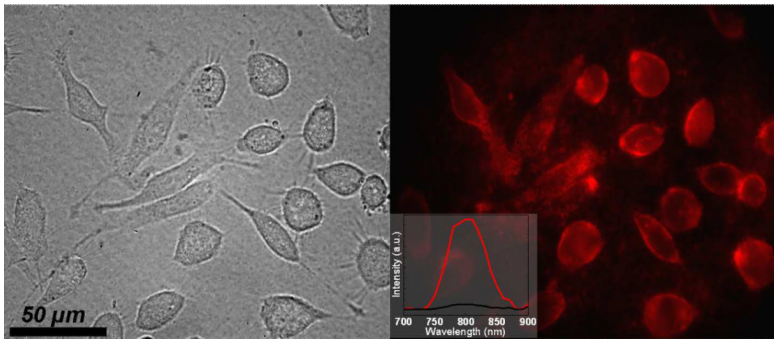


**Figure 4.**

*In vitro* transmission (left) and PL (right) images of Panc 1 cells treated with UCNPs. Inset shows localized PL spectra taken from cells (red) and background (black).

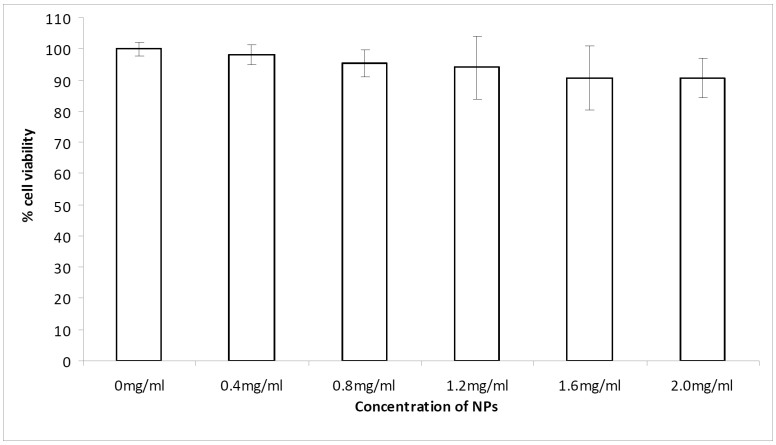


**Figure 5.**
Cell viability assay with Panc 1 cell treated with different concentration of UCNPs.

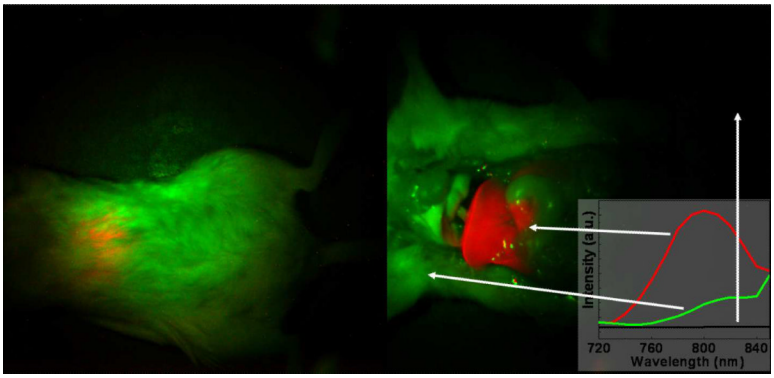


**Figure 6.**

Whole body images of mouse injected i.v. with UCNPs; intact mouse (left), same mouse after dissection (right). The red color indicates emission from UCNPs, green and black show background as indicated by the arrows. The inset presents the PL spectra corresponding to the spectrally unmixed components of the multispectral image obtained with the Maestro system (see supporting information).